Molecular Neurobiology (2019) 56:1957–1971
https://doi.org/10.1007/s12035-018-1202-x

Effects of Prion Protein on Aβ42 and Pyroglutamate-Modified AβpE3-42 Oligomerization and Toxicity

Katiuscia Pagano[1] · Denise Galante[2] · Cristina D'Arrigo[2] · Alessandro Corsaro[3] · Mario Nizzari[3] · Tullio Florio[3] · Henriette Molinari[1] · Simona Tomaselli[1] · Laura Ragona[1]

Received: 10 April 2018 / Accepted: 26 June 2018 / Published online: 6 July 2018

Abstract

Soluble Aβ oligomers are widely recognized as the toxic forms responsible for triggering AD, and Aβ receptors are hypothesized to represent the first step in a neuronal cascade leading to dementia. Cellular prion protein (PrP) has been reported as a high-affinity binder of Aβ oligomers. The interactions of PrP with both Aβ42 and the highly toxic N-truncated pyroglutamylated species (AβpE3-42) are here investigated, at a molecular level, by means of ThT fluorescence, NMR and TEM. We demonstrate that soluble PrP binds both Aβ42 and AβpE3-42, preferentially interacting with oligomeric species and delaying fibril formation. Residue level analysis of Aβ42 oligomerization process reveals, for the first time, that PrP is able to differently interact with the forming oligomers, depending on the aggregation state of the starting Aβ42 sample. A distinct behavior is observed for Aβ42 1-30 region and C-terminal residues, suggesting that PrP protects Aβ42 N-tail from entangling on the mature NMR-invisible fibril, consistent with the hypothesis that Aβ42 N-tail is the locus of interaction with PrP. PrP/AβpE3-42 interactions are here reported for the first time. All interaction data are validated and complemented by cellular tests performed on Wt and PrP-silenced neuronal cell lines, clearly showing PrP dependent Aβ oligomer cell internalization and toxicity. The ability of soluble PrP to compete with membrane-anchored PrP for binding to Aβ oligomers bears relevance for studies of druggable pathways.

Keywords Alzheimer disease · Cellular prion protein · Amyloid beta peptides · Nuclear magnetic resonance · Interaction studies · Cell internalization

Abbreviations

AD	Alzheimer disease
PrP	Cellular prion protein
HM	High monomer content
LM	Low monomer content
NMR	Nuclear magnetic resonance
ThT	Thioflavin
TEM	Trasmission electron microscopy
MTT	3-(4,5-dimethylthiazol-2-yl)-2,5-diphenyltetrazolimu bromide
DMSO	Dimethyl sulfoxide

Electronic supplementary material The online version of this article (https://doi.org/10.1007/s12035-018-1202-x) contains supplementary material, which is available to authorized users.

✉ Simona Tomaselli
simona.tomaselli@ismac.cnr.it

✉ Laura Ragona
laura.ragona@ismac.cnr.it

[1] Istituto per lo Studio delle Macromolecole (ISMAC), CNR, Milan, Italy

[2] ISMAC, CNR, Genoa, Italy

[3] Section of Pharmacology, Department of Internal Medicine, and Center of Excellence for Biomedical research (CEBR), University of Genoa, Genoa, Italy

Introduction

Soluble Aβ oligomers are widely recognized as the principal toxic forms of Aβ peptide, responsible for triggering AD pathophysiology [1–3]. Aβ1-42 peptide (Aβ42) appears to be the earliest form to accumulate in the brain and its free levels in CSF drop long before clinical symptoms [4]. This initial species can be modified over time into a complex array of truncated, isomerized, and/or phosphorylated peptides. One important, highly amyloidogenic and less-studied variant, is the N-truncated pyroglutamate-modified AβpE3-42 peptide, which is devoid of D1 and A2 and cyclized at E3 [5–7] Pyroglutamate-modified variant (AβpE3-42) represents up to 45% of the total

Aβ in senile plaques [8, 9]. Moreover, AβpE3-x peptides were detected in the core of amyloid aggregates in vivo, leading to the hypothesis that AβpE deposition plays a central role in initiating the aggregation of full-length Aβ [5, 10].

Soluble Aβ oligomers are most potent in creating synaptic dysfunction, and Aβ oligomers receptors are hypothesized to be the first step in a neuronal cascade leading to pathology. Indeed, a number of cell surface proteins have been reported as Aβ binding proteins, and cellular prion protein (PrP) has been described as a high-affinity binder of oligomeric Aβ, participating in both physiological and pathological associated events [11]. The vast majority of mature PrP molecules are tethered to the outer leaflet of the plasma membrane through a glycosyl-phosphatydil inositol anchor [12] and lack an intracellular domain for transferring signals from the extracellular environment to the intracellular milieu. Although the role of PrP in AD has been highly debated [13, 14], it is now accepted that it can form complexes with different coreceptor partners on the plasma membrane in order to trigger signaling pathways involved in neuronal differentiation [11], thus playing a critical role in mediating the synaptic deficits induced by Aβ oligomers [15]. The discovery of PrP as a cell surface receptor, selective for Aβ oligomers, has attracted major interest in research focusing on the identification of downstream effectors that mediate the neuronal toxicity and synaptic dysfunction in AD [11, 16]. Specifically, PrP and metabotropic glutamate receptor 5 (mGluR5) may act as coreceptors for Aβ oligomers and have been shown to modulate toxicity and neuronal death in Alzheimer's disease [17–19]. Experiments with neuronal cell culture indicated that the soluble (i.e., glycophosphatidylinositol anchor-free) prion protein and its N-terminal fragment have a strong effect on the aggregation pathway of Aβ42, delaying its assembly into amyloid fibrils [20–22].

In this context, the present paper aims at addressing the characterization, at a molecular level, of PrP interactions with Aβ oligomers, focusing on the effects of these interactions on Aβ42 and AβpE3-42 peptides, still largely unexplored. Furthermore, the neuronal response upon PrP/Aβ oligomers complex formation has been investigated. A combined approach including biophysical methods (NMR, fluorescence, TEM) and cellular validation assays, performed on neuronal A1 cell lines, Wt and silenced for PrP, has been employed to investigate the interactions of human prion protein with the mentioned Aβ peptides and highlight the effects of PrP downregulation.

Thioflavin T (ThT) fluorescence and NMR experiments, employed to investigate the effect of PrP on Aβ aggregation, provide complementary information. ThT increased emission against time reflects amyloid formation [23], while the NMR peak intensity decrease with time is a direct and sensitive measure of the conversion of soluble monomeric species into NMR-invisible assemblies [24]. NMR and ThT fluorescence experiments indicated that PrP can bind both Aβ42 and AβpE3-42 oligomers, delaying their conversion to fibrils. The oligomerization process of ^{15}N-Aβ42 samples, containing different amounts of monomeric species, was simultaneously monitored by NMR in the absence and in the presence of soluble PrP, revealing that PrP exerts a different role depending on the relative ratio of low and high molecular weight species in the starting samples. Furthermore, this analysis revealed, for the first time, that the 1-30 region of Aβ42 is the locus of interaction with the prion protein.

Cellular experiments clearly show that PrP mediates Aβ neurotoxic effect acting as a cell surface receptor that binds Aβ oligomers and favors toxic oligomers internalization and intracellular accumulation. Additional experiments show that soluble PrP efficiently competes with membrane-anchored PrP for interacting with Aβ oligomers.

Materials and Methods

Materials ^{15}N-Aβ42 was purchased from rPeptide; unlabeled Aβ42 and AβpE3-42 were purchased from Anaspec. The analyzed samples were prepared employing recombinant ^{15}N-Aβ42 peptides from the same batch. Unlabeled and ^{15}N labeled human PrP(90-231) were purchased by ASLA Biotech. Human PrP (90-115) and PrP (116-142) were purchased by DG Peptides (Hangzhou China). Thioflavin T was purchased from Sigma-Aldrich.

The following antibodies have been employed: Anti PrP 3F4 (Signet Lab, London, UK); β-Actin Antibody #4967 (Cell Signaling); β-Amiloid (D3D2N) (Cell Signaling). Secondary antibodies: Alexa Fluor 488-conjugated anti-mouse secondary Ab (Molecular Probes, Invitrogen Corp., Carlsbad, CA, USA), for immunocytofluorescence, and horseradish peroxidase-linked anti-mouse or anti-rabbit IgG antiserum (GE Healthcare, Milano Italy) for Western blots.

Aβ Sample Preparation for Fluorescence Measurements Lyophilized synthetic peptide was dissolved in DMSO to a concentration of 220 μM. Aliquots of 75 μL were lyophilized and stored at − 20 °C until used. For all experiments, stock peptides were reconstituted as reported [25]. The concentration of the peptide in the stock solution was estimated by UV using the molar extinction coefficient at 214 nm (ε_{214} = 1490 M^{-1} cm^{-1}) [26].

The stock solution of each peptide was divided in two aliquots. One was diluted to 8 μM in 30 mM phosphate buffer at pH 7.2 to make the reference sample, the other was diluted in 30 mM phosphate buffer at pH 7.2 containing the appropriate amount of PrP.

Thioflavin T Fluorescence Spectroscopy Aβ peptides (8 μM) were incubated at 25 °C in the presence/absence of PrP at Aβ:PrP 1:1 ratio and analyzed in parallel. ThT fluorescence

was followed over time during aggregation. For this purpose, 47.5 μL of each sample were mixed with 2.5 μL of a 400 μM ThT solution in a 3 mm fluorescence cuvette. ThT fluorescence was measured at excitation and emission wavelengths of 440 and 482 nm, respectively. ThT fluorescence data were plotted as a function of time and fitted by a sigmoidal curve described by the following equation [27]: $y = y_i + \frac{y_f - y_i}{1+e^{(t-t_0)k_{\mathrm{fib}}}}$, where y_i and y_f are the initial and final ThT fluorescence, respectively and k_{fib} is the fibril growing rate, t is time, and t_0 is the time to 50% of maximal fluorescence. The lag time is derived as t_0–$2/k_{\mathrm{fib}}$.

Transmission Electron Microscopy (TEM) Aβ peptides (8 μM) were separately co-incubated at 25 °C for 48 h in sterile microtubes with PrP at Aβ:PrP 1:1 molar ratio. Five microliters of each sample were adsorbed for 5 min onto carbon-coated 300-mesh copper grids, in order to evaluate the morphology and the sizes of the species in the different samples. The aggregates species were negatively stained for 1 min with 5 μL of 1% uranyl acetate. All air-dried specimens were examined with a Zeiss LEO 900 electron microscope (Zeiss, Stuttgart, Germany) operating at 80 kV. Images flattening and analysis was performed by the ImageJ software.

NMR Sample Preparation The Aβ42 and AβpE3-42 peptides were prepared in monomeric form as described [28, 29]. In brief, peptides were dissolved in 1,1,1,3,3,3-hexafluor-2-propanol (HFIP), vortexed for 1 min, and after evaporation of HFIP, they were dissolved in DMSO. The peptides were treated by a desalting column and eluted in a 30 mM phosphate buffer pH 7.2, 1 mM EDTA. The samples were kept on ice until required, and the elapsed time before NMR measurement was 30 min. This protocol was employed for all NMR samples. Peptide concentration was verified by UV before and after each NMR measurement, in order to check that no precipitation had occurred during the experiment.

NMR Experiments NMR experiments were performed at 25 °C. Aβ concentration varied from 3 to 20 μM (monomer concentration) in a 30 mM phosphate buffer at pH 7.2 supplemented with 5% (*v*/*v*) D_2O (> 99.96% Sigma-Aldrich). Aβ 20 μM samples were employed for the interaction experiments with PrP. Spectra were acquired on a Bruker DMX operating at 600 MHz and on a Bruker Avance II operating at 500 MHz. 1D NMR experiments were performed at different time points of the kinetics measurements to check that no sample degradation took place.

To detect the influence of PrP on Aβ aggregation kinetics, each Aβ sample was split in two tubes, one was added with PrP protein at 1:1 stoichiometric ratio (holo) and one was added with buffer (apo) (to obtain the same concentration in the two samples), and simultaneously observed on two NMR spectrometers. All the experiments were performed consistently permuting the samples and the spectrometers, in order to have the apo or holo data acquired on both spectrometers.

Kinetics studies were performed on Aβ42 samples by acquiring ^{15}N-HSQC spectra over time to monitor the loss of NMR signal due to aggregation. Gradient-tailored excitation was employed for water suppression to reduce signal losses for exchangeable protons [30, 31].

The decays of NMR peak intensities with time are inverted sigmoidal plots, which can be fitted with an empirical sigmoidal function [24, 27] as follows:

$$y = (a + k_{\mathrm{nucl}} * t) / \left(1 + e^{\left(-k_{\mathrm{growth}}(t-t_0)\right)}\right), \quad (1)$$

where y is the normalized NMR cross-peak intensity, a is the initial intensity, k_{nucl} is the nucleation rate accounting for peak intensity slow decrease, visible in the first part of the transition, k_{growth} describes the maximal rate of self-assembly to NMR-invisible oligomeric species, and t_0 is the midpoint of the sigmoidal transition.

^{15}N-HSQC-based experiments for measuring ^{15}N transverse relaxation were acquired on Aβ42 samples with low monomer content (vide infra), at two relaxation delays of 16 and 400 ms, with a recycling delay set to 3 s.

The kinetics of AβpE3-42 truncated peptide alone and in presence of the ^{15}N-PrP at 1:1 stoichiometric ratio was followed as well, through the acquisition of 1D ^{1}H NMR experiments to follow AβpE3-42 alone and 1D ^{1}H-^{15}N filtered experiments [32] to monitor the aggregation of the unlabeled peptide in the presence of ^{15}N-labeled prion protein. All data were processed using NMRPipe [33] and analyzed with the NMRView software [34]. Each cross-peak volume was normalized with respect to the average cross-peak volume, measured in the relative spectrum, to properly compare different NMR data sets. The relative monomer concentration of different samples was estimated from the total intensity of methyl resonances in 1D ^{1}H spectra with respect to EDTA reference signal.

Cell Cultures Neuronal Mes-c-myc A1 (hereafter A1) cell line was generated from mouse embryonic mesencephalic primary culture. Phenotypical characterization and the demonstration that A1 cells, upon differentiation, retain neuronal features was described elsewhere [35]. A1 cells were cultured in MEM/F12 (Gibco-BRL, Milan, Italy) supplemented with 10% FBS (Invitrogen, USA).

Stable Silencing of PrP Expression in A1 Cell Cultures (A1-PrP-KO Cells) A1 cells were transfected with PrP shRNA Plasmid (h) (Santa Cruz Biotechnology, Santa Cruz, CA, USA), a pool of three target-specific lentiviral vector plasmids each encoding 19–25 nt (plus hairpin) shRNAs, designed to knock-down gene expression, as reported [36]. PrP silencing was evaluated by both RT-PCR and Western blot.

qRT-PCR. Total RNA was extracted using the High Pure RNA Isolation Kit (Roche) and reverse transcribed into cDNA using the iScript cDNA Synthesis Kit (Bio-Rad). Single-stranded cDNA products were analyzed by real-time PCR using the SsoFastTM EvaGreen mix (Bio-Rad) on a CFX96 Touch real-time PCR (Bio-Rad). Cycling conditions were set at 94 °C for 30 s, 60 °C for 30 s, and 72 °C for 30 s, for 37 cycles. Levels of target gene mRNA in each sample were normalized on the basis of GAPDH and 28S amplification and reported as relative values.

Western Blot Cells were lysed in a buffer containing 20 mM Tris-HCl pH 7.4, 140 mM NaCl, 2 mM EDTA, 2 mM EGTA, 10% glycerol, 1% NP-40, 1 mM dithiothreitol, 1 mM sodium orthovanadate, 1 mM phenylmethylsulphonyl fluoride, and the "complete" protease inhibitor cocktail (Roche, Monza, Italy), as reported [37]. Twenty-five micrograms of proteins from each sample were probed with the primary antibodies followed by secondary antibody (horseradish peroxidase-linked anti-mouse IgG antiserum, GE Healthcare, Milano, Italy). Antibody-reactive bands have been detected by ECL (GE Healthcare) using ChemiDoc™ MP Systems (Bio-Rad, Segrate, Italy).

Cell Viability Determination of A1 Neuron Cultures Mitochondrial activity, as index of cell viability, was evaluated by measuring the reduction of 3-(4,5-dimethylthiazol-2-yl)-2,5-diphenyltetrazolium bromide (MTT, Sigma-Aldrich). After treatments, cells were incubated with MTT (0.25 mg/mL) for 1 h, formazan crystals dissolved in DMSO and absorbance measured at 570 nm [38].

Cell Counting Cells were harvested by trypsin-EDTA and the cell suspension diluted 1:10 in sterile PBS and mixed with equal volume of 0.4% Trypan Blue solution to evaluate cell viability. The ratio of live/dead cells was evaluated using an automated cell counter (TC20, Bio-Rad Laboratories, Inc., Hercules, CA), as reported [25]. Data were obtained by three independent experiments performed in quadruplicate. Statistical analysis was performed by means of one-way ANOVA using the "Newman-Keuls multiple comparison post-hoc test."

Immunocytofluorescence Detection of Aβ Internalization A1 Wt and A1-PrP-KO cells, grown on glass coverslips, were treated with Aβ42 (1 μM) or AβpE3-42 (1 μM) for 24 h and fixed with 4% paraformaldehyde, washed in PBS (pH 7.4), and treated with 0.1 M glycine and Triton X-100 (0.1% in PBS). After incubation with β-amyloid (D3D2N) primary antibody (Cell Signaling) for 1 h at r.t., secondary Alexa Fluor 488 anti-mouse antisera (1:200; Molecular Probes, Invitrogen, Milano, Italy) were added for 1 h at r.t. Nuclei were counterstained with DAPI (blue) and cell morphology evidenced by staining with Dil, a lipophilic red-fluorescent dye that binds to cell membranes [39]. Aβ internalization was quantified using the ImageJ software (https://imagej.nih.gov/ij).

Results

PrP Interferes with Fibril Growth Kinetics of Aβ42 and AβpE3-42 The effect of prion protein on Aβ fibrillation process was followed by fluorescence using ThT, a probe that gives strong fluorescence upon binding to β-sheet containing amyloid fibrils [23]. The 90-231 region of PrP (hereafter simply referred to as PrP), including the 95-111 region, reported as the major epitope for Aβ oligomers binding [15, 40–42], was chosen as a model to investigate in vitro and *in cell* interactions with Aβ oligomers. The results of the ThT assays, simultaneously run for Aβ peptides with and without PrP, obtained in solution conditions different from those previously reported in the literature [43–46], are shown in Fig. 1. ThT kinetics recorded for PrP alone indicates that no contribution to ThT fluorescence comes from PrP (Fig. S1).

The presence of prion protein lengthens the lag phase of both Aβ42 and AβpE3-42 peptides, leaving the fibril growth rate substantially unaffected (Fig. 1c, d). The final quantity of β-sheet structure, as deduced from the measured emission (plateau of the curve), is lower in the presence of prion protein.

Morphological Studies on Aβ42 and AβpE3-42 without and with Prion Protein The morphological analysis of *A*β peptides alone or in the presence of PrP is reported in Fig. 2. Panel a shows long curvilinear entangled fibrils typical of *A*β42 samples. The amount of fibrils observed for Aβ42 alone (panel a) significantly decreases in the presence of PrP (panel b). Panel d shows AβpE3-42 morphology, characterized by few protofibrils and many amorphous aggregates.

In line with the behavior observed for *A*β42, the presence of PrP causes an important decrease of AβpE3-42 amorphous aggregates sizes and a disappearance of protofibrils (panel e). It is important to note that PrP alone does not form fibers, as shown in panel c. Only little amorphous aggregates are present, indicating that, in our conditions, PrP is stable and does not aggregate in beta-sheet conformation, typical of fibrils.

Residue Level Analysis of Aβ42 Oligomerization Kinetics by NMR: the Role of PrP The NMR resolving power was exploited to probe the molecular details of the oligomerization process, on a per-residue basis, following the behavior of single ^{15}N-Aβ42 residues, by recording a series of ^{15}N-HSQC spectra over time, in the presence and absence of unlabeled PrP. A Aβ42:PrP stoichiometric ratio of 1:1 was employed to compare the binding information obtained with our PrP construct with data reported in the literature for other constructs

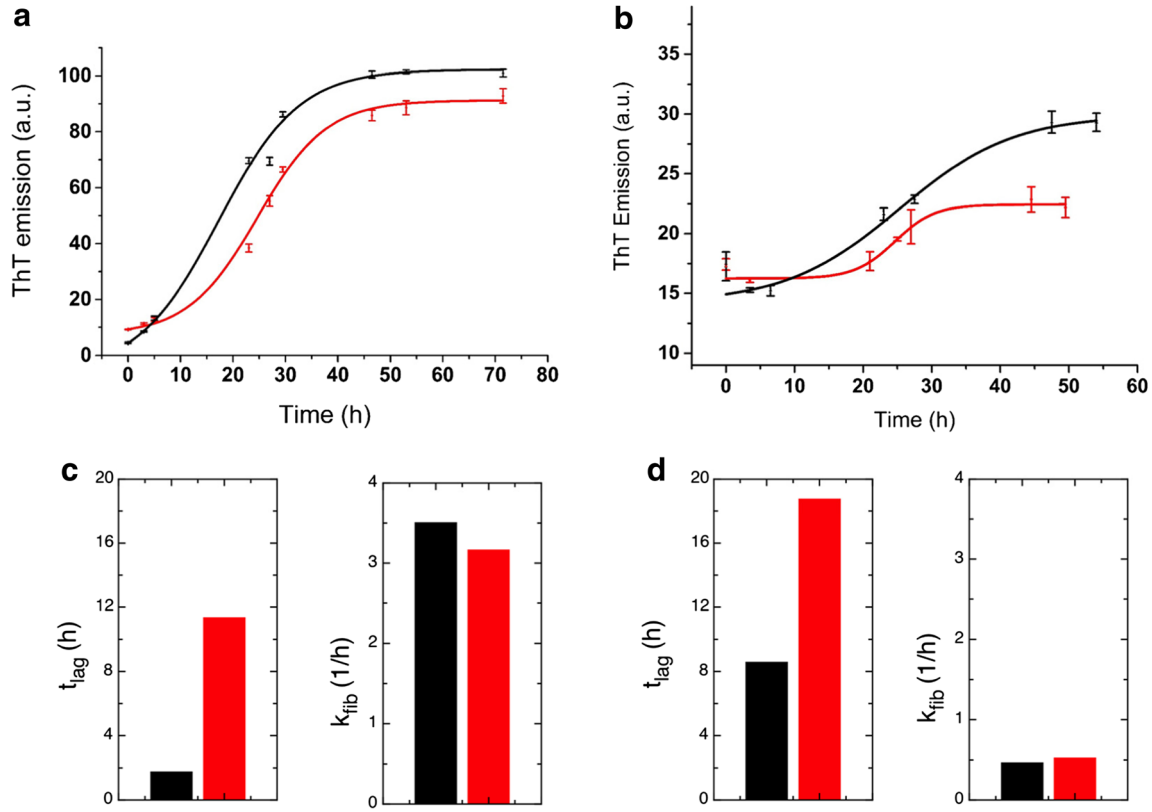

Fig. 1 ThT fluorescence in the presence of Aβ peptides, without and with PrP. Data obtained for 8 μM Aβ42 without (black) and with PrP at Aβ42:PrP 1:1 (red) ratio in a 30mM phosphate buffer, 25 °C are reported in panel (**a**). Data obtained for AβpE3-42 in the same experimental conditions are reported in panel (**b**) with the same color code. Error bars refer to standard deviation on measurements done in triplicate on three different freshly prepared samples. Histograms summarize the results of the fitting to a sigmoidal curve (see Materials and Methods). Fibril growth rate (k_{fib}) and lag time (t_{lag}) obtained from Aβ42 and AβpE3-42 data fitting are reported in panels (**c**) and (**d**), respectively. The same color code of panels (**a**) and (**b**) is used

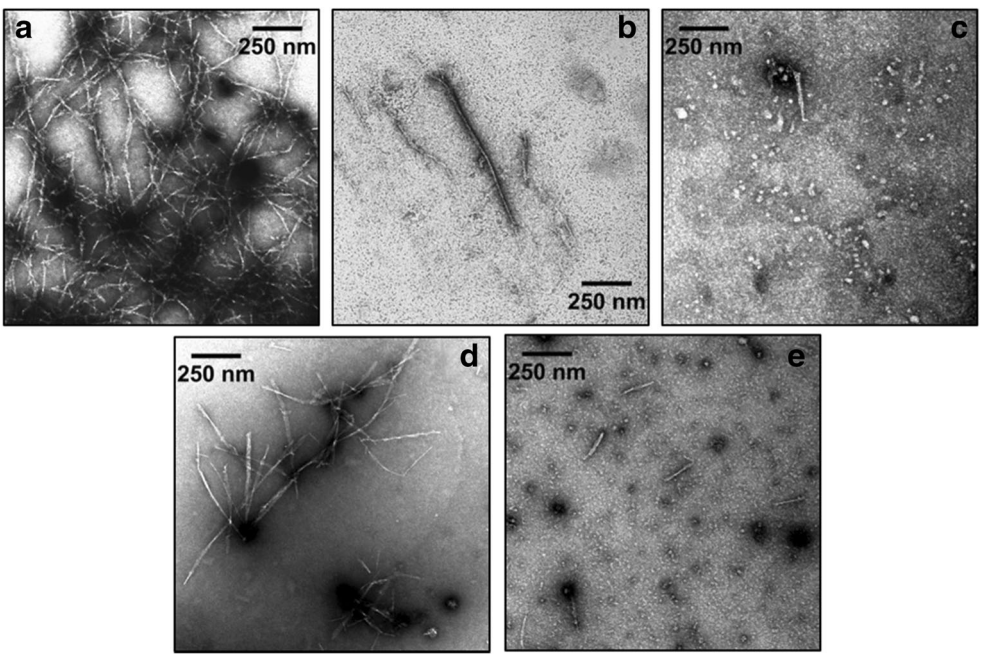

Fig. 2 TEM micrographs of Aβ after 48 h of aggregation at 25 °C, in 30 mM phosphate buffer pH 7.2, in presence or in absence of PrP. (**a**)Aβ42; (**b**) Aβ42:PrP 1:1; (**c**) PrP; (**d**) AβpE3-42; (**e**) AβpE3-42:PrP 1:1

[15, 20, 21, 47, 48]. It should be noted that we recorded data in the presence of a large excess of PrP in order to ensure complete Aβ oligomer saturation, on the basis of PrP/Aβ affinity data [47].

The kinetics of the conversion of monomers to high molecular oligomeric species can be followed monitoring the disappearance of peptide resonances, due to the increased molecular weight of the formed oligomers. Indeed, NMR resonances disappear as a consequence of the formation of heterogeneous high molecular weight aggregates, also referred to as "NMR-invisible species," which tumble slowly in solution on the NMR time-scale and give rise to signals that are too broad to be directly observed by conventional liquid state NMR experiments.

The comparison of the aggregation kinetics in the presence and in the absence of prion protein should however take in consideration the Aβ samples variability, which strongly affects the process of fibril formation. Such variability was reported to be strongly dependent upon the specific conditions (ionic conditions, pH, temperature, vortexing time), the manufacturing route (synthetic or recombinant), and the methods of synthesis, purification, and storage [49]. In our hands, sample variability was still observed, despite using the same recombinant peptide batch, treated with the same protocol, as exemplified in Fig. S2, reporting selected examples of Aβ42 decaying kinetic curves. As some of the controversy in the literature data on the interaction between PrP and Aβ peptides may derive from this sample variability [50], each Aβ sample was split in two (with and without PrP) and simultaneously observed on two NMR spectrometers. This spectrometer-time consuming approach ensures the reliability of the data, since the kinetics of each Aβ-PrP complex can be compared to the kinetics of the corresponding apo Aβ sample.

The main NMR observable species in the ^{15}N-HSQC spectrum of ^{15}N-Aβ42 samples is the monomer in consideration of the concentration (~ 20 μM) of the starting Aβ42 sample [51, 52] and of the reported literature data on the transient nature of oligomeric species [53, 54]. Addition of PrP to ^{15}N-Aβ42, at equimolar ratio, does not induce any Aβ42 chemical shift and linewidth variation. Minor peak intensity changes are observed, whereas no new resonance appears in the spectra (Fig. S3). The complementary experiments, recorded on ^{15}N-PrP:Aβ42 1:1 sample, evidenced significant intensity variation for several PrP amide resonances upon Aβ42 addition (Fig. S4), supporting the direct interaction of PrP with Aβ42 peptide. The ability of PrP to interact also with AβpE3-42 peptide is demonstrated by the peak intensity changes observed in HSQC spectra recorded for the ^{15}N-PrP:AβpE3-42 1:1 sample (Fig. S4). Altogether, the NMR data suggest that PrP preferentially interacts with the heterogeneous mixture of unstable oligomers of varying sizes and conformational states [55], rather than with the monomer, in agreement with literature data [20, 47].

The aggregation kinetics of apo Aβ42 can be analyzed at a per-residue level, measuring the decrease of NMR cross-peak intensity of each resonance in the ^{15}N-HSQC spectra, as a function of time. The analysis of Aβ42 aggregation kinetics in the presence of PrP revealed the presence of two different scenarios, depending on the oligomerization state of the starting apo Aβ42 sample. When PrP is added to an Aβ42 sample with "high monomer content" (HM), selected residues, located at the 1-30 region, remain visible and retain their NMR signal intensity (Fig. 3a), even when the resonances of the C-terminal tail disappear, following the expected sigmoidal curve due to aggregation into NMR-invisible species (Fig. 3b). The observed local differential behavior is clearly evinced from the comparison of resonance intensities at the beginning and at the end of the kinetic curve (Fig. 3c) and is summarized on the monomer structural model [56] (Fig. 3d). This NMR observation is consistent with PrP interaction with Aβ42 growing oligomers, specifically involving Aβ42 N-tail residues. This region is thus protected from further oligomerization, which is known to be driven by Aβ42 C-terminal tail [7, 57, 58].

When PrP is added to a "low monomer content" (LM) Aβ42 sample, a concerted resonance intensity decrease is observed for all the residues (Fig. 3e, f). We reasoned that in the LM sample, highly mobile residues, belonging to 1-30 region, are no more available for a specific interaction with prion protein, and higher molecular weight preformed oligomeric species interact with prion protein.

The analysis of the aggregation curves of single Aβ42 residues indicated that no significant fluctuation was found on the kinetic parameters (nucleation rate, lag duration, growth rate) along the amino acid sequence. The sum of all NMR intensities of ^{15}N-HSQC resonances was therefore used to probe the peptide aggregation kinetics. PrP addition to both HM and LM Aβ42 samples, significantly affected the nucleation rate (Fig. 4b, e), while minor effects were instead observed for the growth rate (Fig. 4c, f). Major effects on the lag phase lengthening were observed for the LM sample (Fig. 4d), whose resonance intensities were completely lost after 20 h in the absence of PrP, and remained observable for up to 100 h after PrP addition.

In order to further investigate the interaction of PrP with Aβ42 oligomers, the changes in ^{15}N transverse relaxation of a LM Aβ42 sample, upon PrP addition, were estimated by recording ^{15}N-HSQC-based experiments at two relaxation delays (16 and 400 ms). It should be noted that a complete T_2 experiment could not be run, as the signal of the apo LM sample is rapidly decaying. In this kind of experiments, the volume of the NMR cross peak is related to the size of the observed species, with larger species decaying faster. Figure 5 reports the cross-peak volume ratios (Vol_{400ms}/Vol_{16ms}) as a function of the residue number. The average volume

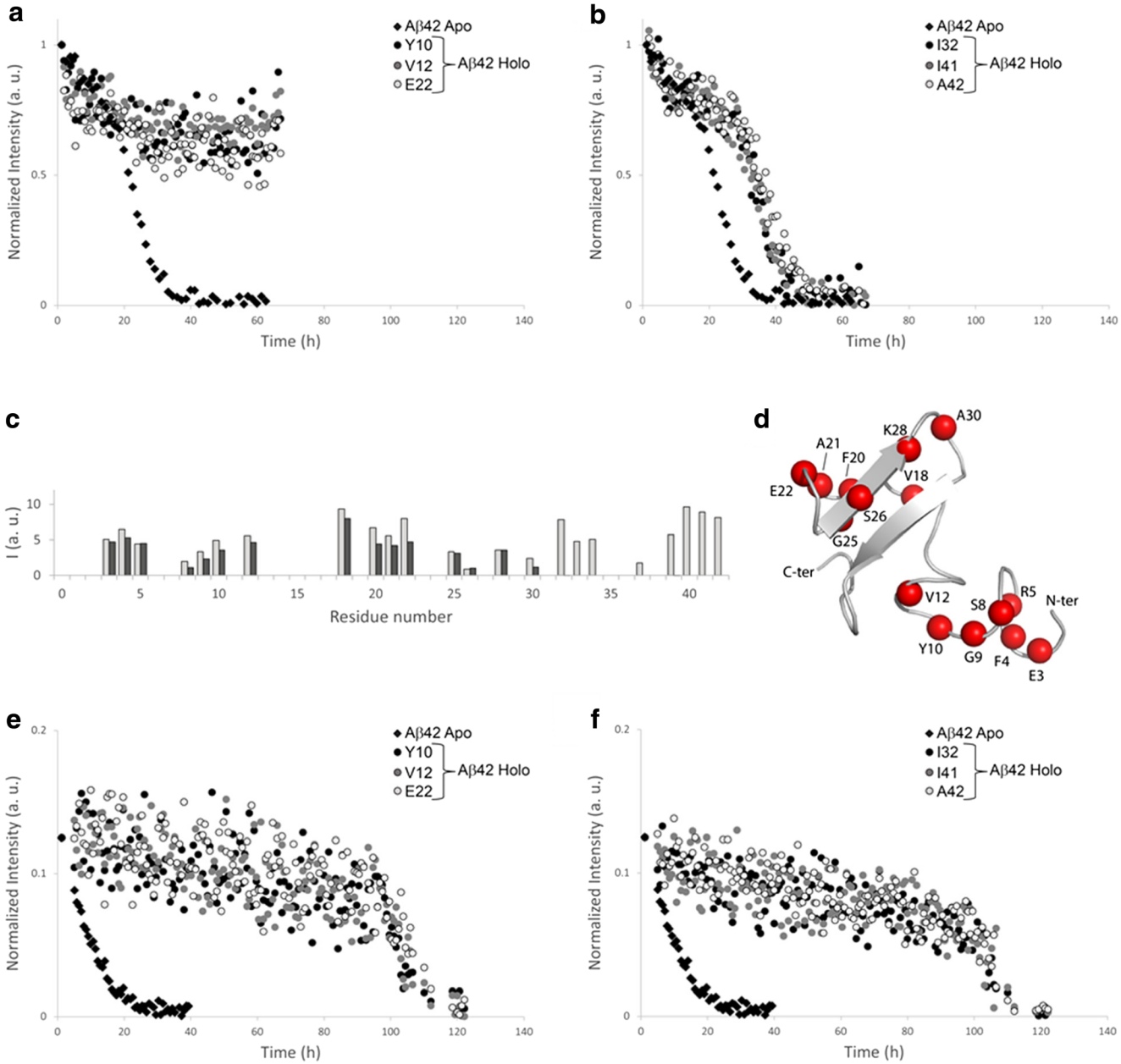

Fig. 3 Residue level analysis of Aβ42 kinetics in the absence and presence of PrP. The kinetic curve of the apo samples are reported as black diamonds and the intensity decay refers to the normalized sum of all peak intensities. The behavior of residues belonging to selected Aβ42 residues (indicated in the panel) belonging to 1-30 (**a**) and C-terminal regions (**b**), in presence of prion protein, as observed for a starting apo sample with "high monomer content" (HM). Comparison of resonance intensity at the beginning (light gray bars) and at the end (black bars) of the kinetic curve is plotted as a function of residue number (**c**). Residues displaying delayed intensity decays in the presence of PrP, as deduced from NMR data, are highlighted as red spheres on the structure obtained by Tomaselli et al. [56] (**d**) The behavior of selected Aβ42 residues (indicated in the panel) belonging to 1-30 and C-terminal regions in the presence of prion protein, as observed for a starting sample with "low monomer content" (LM), is reported in panels (**e**) and (**f**), respectively. The monomer concentration in the LM starting sample was scaled with respect to the HM sample, on the basis of the comparison of the total intensity of methyl resonances in 1D ^{1}H spectra

decreases from 0.36 for the apo peptide to 0.29 for Aβ42 in the presence of PrP.

The observed decrease in the mean value of the volume ratio reflects the presence of exchange between the NMR observable monomeric species and an oligomeric form whose size is increased by the interaction with the PrP (Fig. 5).

Residues R5, K16, F20, E11, G25, G29, G33, and G38 relax very quickly in Aβ42 samples, possibly as a result of exchange contribution. Indeed, in the spectra recorded with the longer delay (400 ms), their peak disappear, causing the volume ratio to become zero. Upon PrP addition, the relaxation rates of R5, K16, and F20 decrease

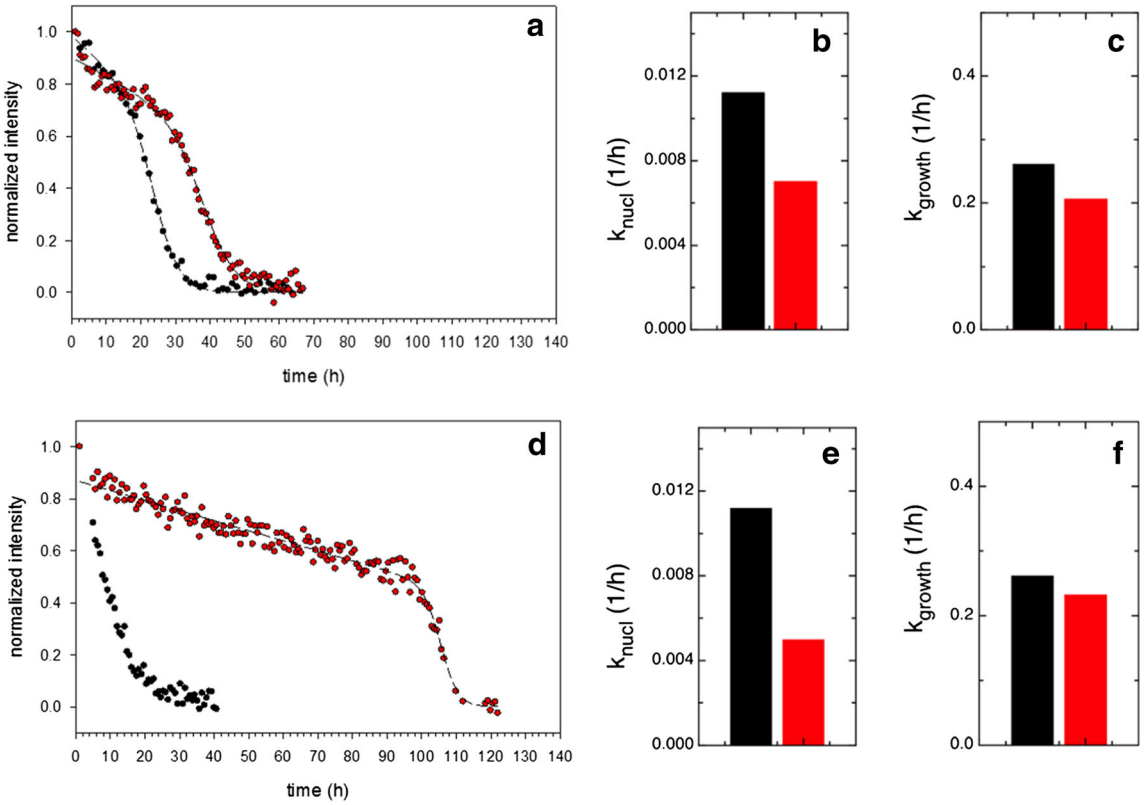

Fig. 4 Oligomerization kinetics of Aβ42 as followed by NMR in the absence and presence of PrP. The sum of cross-peak normalized intensities is reported as a function of time for the HM (**a**) or LM (**d**) starting samples. Black kinetics curves refer to Aβ42 alone, while red curves are obtained in the presence of equimolar amounts of PrP. In panel (**a**), red curve summarizes the behavior of C-terminal residues. Dashed lines represent data fitting to equation $y = (a + k_{nucl}*t)/(1 + \exp(-k_{growth}(t-t_0)))$. The black curve in panel (**d**) could not be fitted with a sigmoidal curve. Fitting values obtained for the nucleation and growth rates deduced from curves reported in (**a**) are summarized in panels (**b**, **c**). In (**e**, **f**) panels, red bars refer to values obtained from fitting of holo data reported in panel (**d**) (red curve), while black bars are the same of panels (**b**, **c**). The color code is the same as in panels (**a**, **b**)

leading to a value, for the volume ratio, close to the average, indicating that they relax as the whole peptide. We expect that when Aβ oligomer is engaged with PrP, these residues experience a different environment, which reduce their conformational exchange. Local stabilizing effects induced by oligomer interaction with PrP are mirrored and measured by NMR on visible monomeric Aβ42, which is exchanging with an oligomer perturbed by PrP presence. These data further support a direct interaction with PrP.

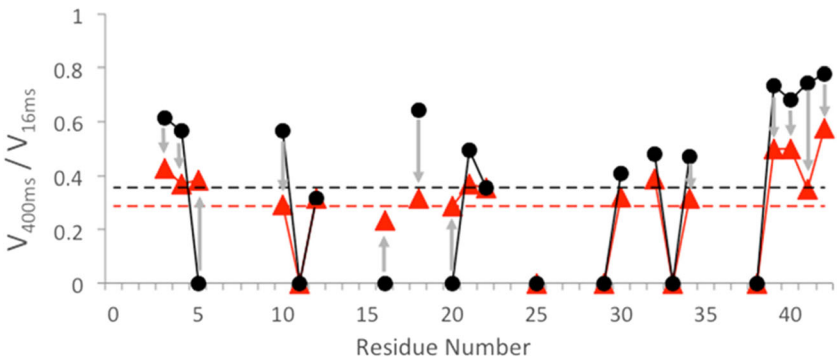

Fig. 5 Transverse relaxation HSQC-based experiments obtained with two different delays (16 and 400 ms) performed on a LM Aβ42 sample upon addition of PrP. The cross-peaks volume ratios (Vol_{400ms}/Vol_{16ms}) obtained for apo (black dots) and holo (red triangles) samples is reported as a function of residue number. The black dashed line at 0.36 represents the average cross-peak volume obtained for apo Aβ42 LM sample, while the red dashed line at 0.29 represents the average cross-peak volume obtained for the holo sample. Gray arrows pinpoint the residues exhibiting marked local changes

Effect of PrP on AβpE3-42 Oligomerization Kinetics by NMR

The kinetics of AβpE3-42 peptide alone and in presence of the ^{15}N-PrP was followed as well, through the acquisition of 1D ^{1}H NMR experiments, to follow apo AβpE3-42, and 1D ^{1}H-^{15}N filtered experiments, to monitor the aggregation of the unlabeled AβpE3-42 in the presence of ^{15}N-PrP (Fig. S5). At variance with apo Aβ42, kinetics data on apo AβpE3-42 indicate that the signal intensity is not completely lost after 80 h, suggesting the presence of different equilibria between monomeric AβpE3-42 and oligomeric states/NMR-invisible states, in agreement with ThT results and reported morphological data [59]. PrP was able to bind and slow down AβpE3-42 oligomerization kinetics, as deduced from the NMR observed intensities, which remained substantially unchanged up to 80 h. Longer kinetics could not be observed due to peptide degradation.

Evaluation of Cellular Response to Aβ Oligomers: Role of PrP

To investigate the cellular response to addition of Aβ42 and AβpE3-42 oligomers, experiments were performed using A1 neuronal cell line, which combines indefinite in vitro proliferation with the retaining of a neuronal phenotype. In fact, most of the reported studies on Aβ oligomers-PrP have been conducted on neurons, and it was reported that Aβ oligomers-PrP binding on neuronal surface is much higher than on glial surface [15]. Aβ42 and AβpE3-42 showed a statistically significant toxic effects in A1 Wt neurons, after only 24 h of treatment, causing a viability reduction of 45 and 50%, respectively, as compared to vehicle-treated controls. This effect was more pronounced after 48 h of treatment (80 and 88% reduction of cell viability for Aβ42 and AβpE3-42, respectively) (Fig. 6). To test the role of PrP in the Aβ toxicity, A1 neuronal cells were silenced for PrP expression (A1-PrP-KO), by PrP shRNA transfecting (Fig. S6). PrP downregulation completely abolished Aβ42 and AβpE3-42-induced toxicity following the same treatment used in A1 Wt (Fig. 6).

These data support the hypothesis that the expression of PrP is required for Aβ42-induced neurotoxicity [15] and show, for the first time, that the same mechanism is shared also by AβpE3-42. On the ground of this evidence, we investigated the mechanism by which PrP can mediate Aβ neurotoxicity.

In particular, considering the ability of PrP to bind Aβ oligomers, as evidenced by NMR data, we tested whether this interaction would lead to Aβ oligomers internalization, in order to confirm the role of the intracellular accumulation as the toxicity determinant.

A1 neurons (Wt and PrP-KO) were treated with Aβ42 or AβpE3-42 peptide, and their internalization was tested by immunocytofluorescence. After treatment, A1 Wt cells display the presence of a significant load of intraneuronal Aβ42 accumulation (Fig. 7a left panel) in about 78% of the cells (Fig. 7c).

Similar results were observed for AβpE3-42 (Fig. 7b, left panel) that accumulates in about 82% of the cells. Conversely, A1-PrP-KO cells exhibit very low internalization of both Aβ peptides (Fig. 7a, b right panels), being detected as intracellular aggregates in about 12 and 14% of the cells treated with Aβ42 and AβpE3-42, respectively (Fig. 7c, d). It is worth noting that Aβ internalization nicely correlates with the cytotoxic activity of the peptides, indicating that their neurotoxicity is dependent on a PrP-mediated intraneuronal accumulation.

To further support the suggestion that Aβ-PrP binding is the pivotal event causing neuronal death, we verified whether the saturation of the molecular sites responsible for Aβ-PrP binding could at least reduce Aβ neurotoxicity. To this aim, we tested the effect of the preincubation (5 h) of Aβ42 or AβpE3-42 with soluble recombinant PrP, which should allow the interaction between the two molecules, and verified

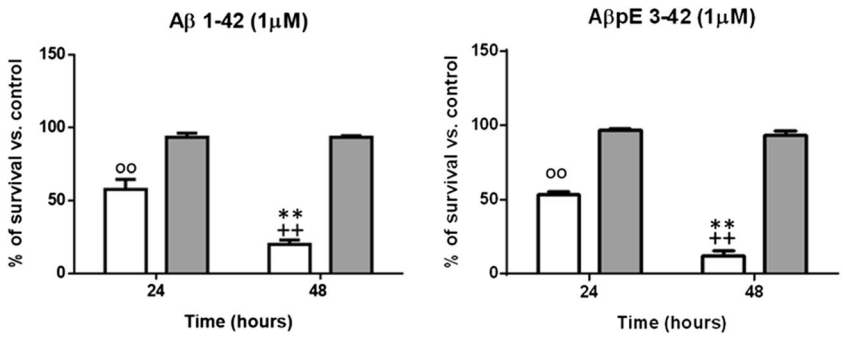

Fig. 6 Viable A1 Wt (white bars) and A1-PrP-KO (gray bars) neurons were evaluated by automated live cell detection (Trypan blue exclusion test) after 24 and 48 h of treatment with both Aβ42 (left panel) and AβpE3-42 (right panel) peptides (1 μM). A1 Wt were plated in a 24-multiwell culture plates at the concentration of 2.5×10^4/well. Data are expressed as percentage of vehicle-treated samples (representing 100%); each point represents the average of three experiments performed in quadruplicate. $^{**}p < 0.001$ vs. 24 h A1 Wt cells; $^{OO} < 0.001$ vs. 24 h A1 PrP-KO cells; $^{++}p < 0.001$ vs. 48 h A1 PrP-KO cells

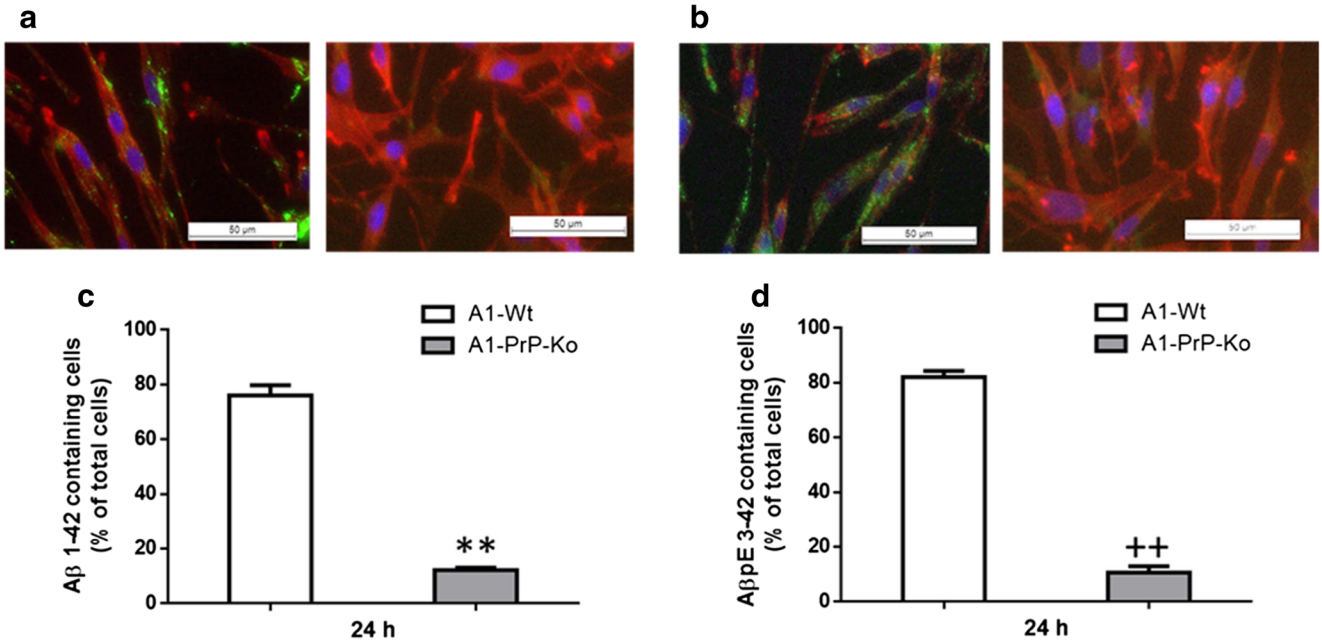

Fig. 7 Aβ42 and AβpE3-42 internalization into A1 Wt or A1-PrP-KO cells. Representative images of Aβ42 (**a**) or AβpE3-42 (**b**) (1 μM) internalization into A1 Wt (green fluorescence in left panels) and A1-PrP-KO (right panels) after 24 h of treatment evidenced as green staining. Nuclei were counterstained with DAPI (blue) and cells morphology was evidenced by staining with the red-fluorescent dye Dil. Data quantification, obtained using the ImageJ software, reports the cells that unambiguously showed intracellular positive clusters of Aβ42 (**c**) and AβpE3-42 (**d**) and are expressed as percentage of total number of cells in three independent microscopic fields ± SEM from three independent experiment. $^{**}p < 0.01$ vs. A1 Wt Aβ42 treated cells; $^{++}p < 0.01$ vs. A1 Wt AβpE3-42-treated cells

whether the peptides were still able to affect A1 neuron viability. The recombinant PrP protein we used is not toxic for neurons in its soluble α-helix rich conformation, as previously shown by some of us [60, 61]. Neuronal viability was tested by MTT reduction assay and by Trypan blue exclusion assay after 24 and 48 h of treatment with Aβ and PrP peptides alone or after preincubation.

After co-incubation with recombinant PrP, which per se did not affect neuronal viability (Fig. 8a, c), both Aβ42 and AβpE3-42 toxicity was partially reduced in A1 Wt neurons reaching a statistically significant effect (Fig. 8a, c). Conversely, toxic effects of Aβ peptides were not detected in A1-PrP-KO neurons, independently from the co-incubation with PrP (Fig. 8b, d). Thus, soluble PrP sequesters Aβ oligomers decreasing the binding to PrP on neuronal membrane and the subsequent internalization and toxicity. In our experimental model, the observed recovery is only partial due to the likely incomplete binding of Aβ oligomers to soluble PrP, leaving a still significant amount of free oligomers able to be internalized and to induce cell death.

PrP residues involved in Aβ binding and mostly responsible for the reduction of Aβ neurotoxic are located in the 90-115 region, as deduced from additional experiments in which two shorter PrP constructs, namely PrP (90-115) and PrP (116-142), were compared (Fig. S7). These results are consistent with previously reported data [15, 62].

Discussion

In the present study, the interactions between Aβ42 and AβpE3-42 peptides and PrP were investigated employing both biophysical (ThT fluorescence, NMR, and TEM) and cellular approaches.

The reported NMR data suggest, in line with previous work [20, 47], a preferential interaction of PrP with Aβ oligomers, rather than monomers. Indeed, Nieznansky et al. [20] clearly showed that the soluble prion protein and its N-terminal fragment have a strong effect on the aggregation pathway of Aβ42, inhibiting its assembly into amyloid fibrils, while Younan et al. [47] identified a specific recognition site on PrP, notably residues 95-113, which binds to Aβ oligomers. The novelty of the NMR data here reported lays in the differential behavior observed for Aβ42 samples, with high and low monomer contents, in their interactions with PrP and the consequent identification of the Aβ42 region involved in the interaction. Discussed data also clarify the evidences in favor of the interaction of PrP essentially with oligomeric Aβ species. However, we cannot rule out the presence of a very weak interaction of PrP with monomeric species, as discussed in the literature [48].

NMR and ThT data indicated that, for both peptides, PrP competed with nucleation and elongation processes, delaying further growth of the NMR-invisible Aβ species and/or fibril.

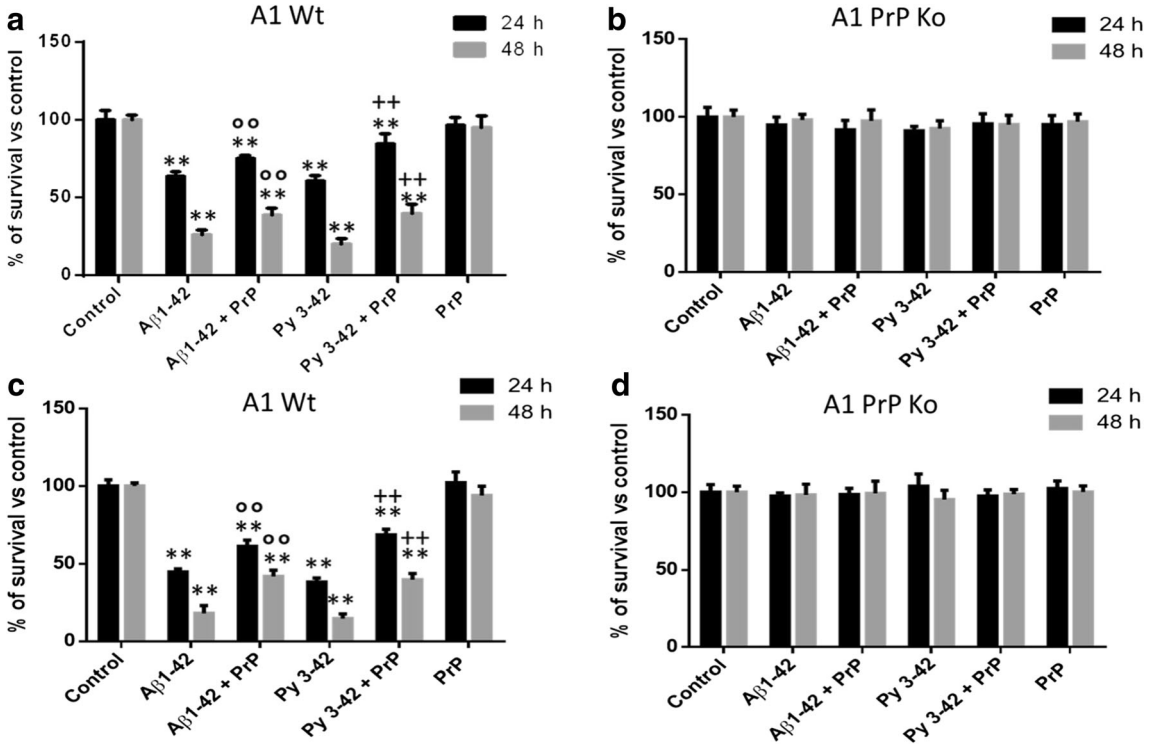

Fig. 8 Aβ42 and AβpE3-42 (1 μM) alone or pre-incubated (5 h at 37 °C) with PrP (1 μM) were added to A1 Wt (**a**, **c**) and A1-PrP-KO (**b**, **d**) cells. Viable cell number was assessed by MTT reduction assay (**a**, **b**) and by automated live cell detection (**c**, **d**) after 24 and (black bars) and 48 (gray bars) hours of treatment. Data are expressed as percentage of vehicle-treated samples (control) and represent the average of three experiments in quadruplicate. $^{**}p < 0.001$ vs. respective controls; $^{OO}p < 0.05$ vs. respective Aβ42-treated cells; $^{++}p < 0.001$ vs. respective AβpE3-42-treated cells

The nucleation phase of Aβ42, as deduced from NMR kinetic analysis, was significantly lengthened in the presence of prion protein, with higher effects for starting samples containing pre-aggregated species. Interestingly, prion protein was also

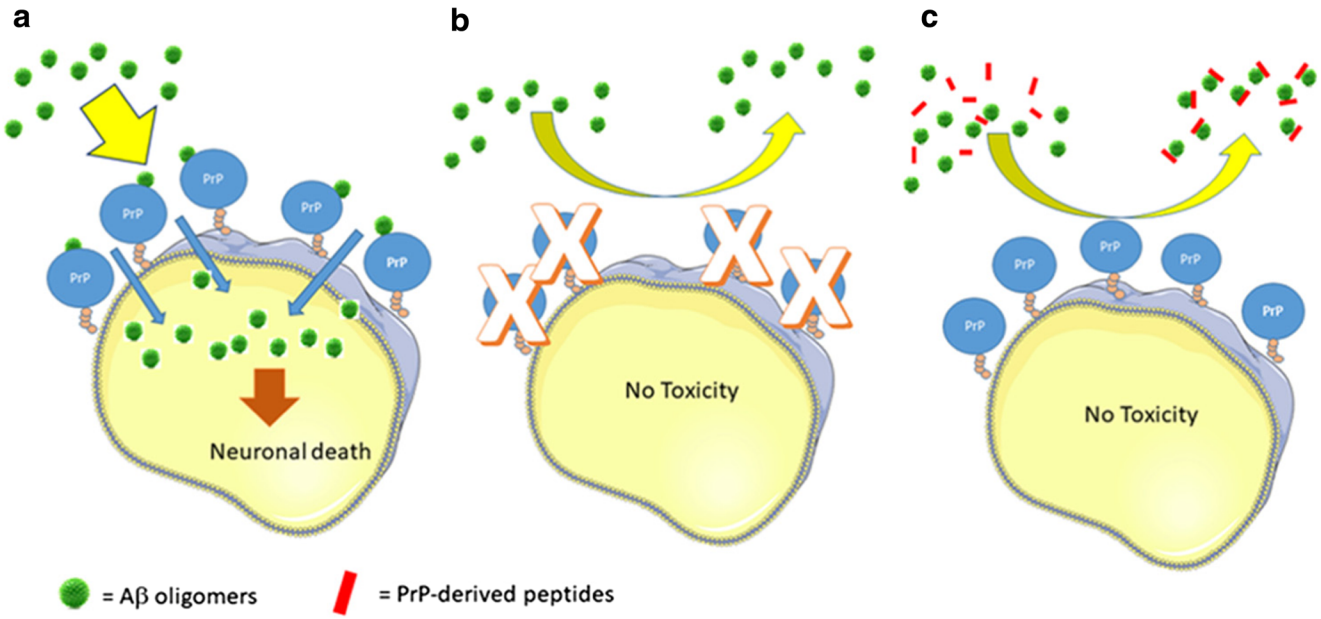

Fig. 9 Proposed model of the role of interaction between Aβ oligomers and PrP in the induction of Aβ-mediated neurotoxicity. (**a**) The binding of the oligomers is required for their internalization causing intracellular accumulation and disruption of protein clearing mechanisms. The prevention of PrP/Aβ oligomer interaction either by PrP silencing (**b**) or saturating possible interacting domains in the presence of PrP-derived peptides (**c**) inhibit Aβ intracellular accumulation impairing its neurotoxicity

effective in interacting with N-truncated AβpE3-42 oligomers, stabilizing for a long time an NMR visible species and reducing the total amount of fibrils, as deduced from ThT fluorescence data. The morphological analysis confirmed that PrP induces a profound change in the structure of both Aβ peptides, decreasing the amount and the interconnections of the fibers.

Cellular tests, performed on A1 Wt and A1-PrP-KO neuronal cell lines, clearly indicated that PrP mediates Aβ42 and AβpE3-42 toxicity through the binding of the peptides and their internalization during the rapid recycle of PrP from the membrane to the cytosol. Indeed, downregulation of PrP prevents Aβ toxicity by hampering the accumulation of toxic concentrations of amyloid peptides within neurons. A relevant outcome of this study is the observed effect on the highly toxic N-terminal pyroglutamate peptide, which has recently gained attention for its exceptionally high amyloidogeneity and neurotoxicity [5], ascribed to its resistance to enzymatic degradation [63]. To the best of our knowledge, the interaction of N-truncated forms with prion protein has never been addressed before.

One of the most important results, derived from the NMR investigation, is that PrP is able to differently interact with the forming oligomers, depending on the aggregation state of the starting sample. When PrP was added to Aβ42 samples at the beginning of the nucleation period, an oligomeric species, characterized by elevated flexibility in the 1-30 region, was stabilized. This result leads us to propose that Aβ42 1-30 region is the locus of interaction with the prion protein. On the contrary, the C-terminal region has a pivotal role in regulating peptide oligomerization. The role of the C-terminus as the initiator core of the aggregation process has its ground in cryo-EM [57] and MAS NMR [58] structural data. Along the same line, our solution NMR data on the interactions between Aβ42 and its N-truncated alloforms also highlighted the C-terminal region of Aβ42 as the locus of initial co-oligomerization [7].

To the best of our knowledge, this is the first report on a per-residue analysis of Aβ42 peptide oligomerization behavior in the presence of PrP. It is thus possible to speculate that either PrP captures and stabilizes a short-lived oligomeric species, or it prevents the 1-30 Aβ tail from entangling on the mature fibril.

Altogether, the data support the hypothesis that cellular prion protein provides high-affinity binding sites for Aβ42 and AβpE3-42 oligomers, inducing changes in the structural and morphological properties of aggregated species.

The comparison of A1 Wt and A1-PrP-KO cellular response to Aβ oligomers addition clearly highlighted the role of membrane-anchored PrP in mediating Aβ cell internalization and toxicity. Thus, we can speculate that, following PrP binding, Aβ oligomers are internalized within neurons where they form insoluble aggregates which, in turn, cause a dysfunction of the lysosome/autophagic response leading to neuronal death (Fig. 9a). This mechanism was already reported for other amyloidogenic peptides [64] and, in particular, for neurotoxic truncated PrP molecules [65, 66]. In this context, the lack of PrP-mediated internalization (using A1-PrP-KO neurons, Fig. 9b) or the inhibition of the binding of Aβ oligomers to PrP, as a result of the saturation of the interacting moiety with synthetic PrP-derived peptides (Fig. 9c), prevent or reduce the neuronal death.

Alternatively, it has been reported that Aβ oligomers bound to lipid-anchored PrP, activate intracellular Fyn kinase to disrupt synapses [67]. The interaction between Aβ oligomers-PrP complex and Fyn cannot be direct, since PrP is anchored via glycolipid to the plasma membrane while Fyn is cytoplasmic. Indeed, it was reported that only co-expression of the glutamate receptor, mGluR5, allowed PrP bound to Aβ oligomers to activate Fyn [68]. Thus, it is possible that Aβ oligomers-PrP complexes at the neuronal surface might activate mGluR5 to disrupt neuronal function. The observed partial recovery of neuronal survival after Aβ oligomers preincubation with soluble PrP could support the requirement of Aβ-PrP interaction at neuronal membrane level.

The elucidation of the molecular interactions of Aβ oligomers with membrane-anchored PrP and soluble PrP sheds light on the recognition and toxicity pathways of the different Aβ peptides, opening the way to the identification of inhibitors directed towards a specific PrP region.

In light of the pivotal role of the Aβ oligomeric state in AD pathophysiology, further work is current in progress, following different approaches [69–72], aimed at the identification of the structural features of the complex formed between early forming Aβ oligomers and PrP.

Funding Information This work was supported by the Alzheimer Association (NIRG-14-321500 Grant) and CARIPLO Foundation (2015-0503). LR, KP, ST acknowledge financial support of University of Verona (Bando JOINT Projects 2017, Prof. Michael Assfalg - Dr. Laura Ragona). KP, HM and LR acknowledge Fondazione Antonio De Marco for financial support.

References

1. Selkoe DJ, Hardy J (2016) The amyloid hypothesis of Alzheimer's disease at 25 years. EMBO Mol Med 8(6):595–608. https://doi.org/10.15252/emmm.201606210
2. Ono K (2017) Alzheimer's disease as oligomeropathy. Neurochem Int. https://doi.org/10.1016/j.neuint.2017.08.010
3. Forloni G, Artuso V, La Vitola P, Balducci C (2016) Oligomeropathies and pathogenesis of Alzheimer and Parkinson's diseases. Mov Disord 31(6):771–781. https://doi.org/10.1002/mds.26624
4. Bateman RJ, Xiong C, Benzinger TL, Fagan AM, Goate A, Fox NC, Marcus DS, Cairns NJ et al (2012) Clinical and biomarker changes in dominantly inherited Alzheimer's disease. N Engl J Med 367(9):795–804. https://doi.org/10.1056/NEJMoa1202753
5. Cynis H, Frost JL, Crehan H, Lemere CA (2016) Immunotherapy targeting pyroglutamate-3 Abeta: prospects

and challenges. Mol Neurodegener 11(1):48. https://doi.org/10.1186/s13024-016-0115-2
6. Nussbaum JM, Schilling S, Cynis H, Silva A, Swanson E, Wangsanut T, Tayler K, Wiltgen B et al (2012) Prion-like behaviour and tau-dependent cytotoxicity of pyroglutamylated amyloid-beta. Nature 485(7400):651–655. https://doi.org/10.1038/nature11060
7. Tomaselli S, Pagano K, D'Arrigo C, Molinari H, Ragona L (2017) Evidence of molecular interactions of Abeta1-42 with N-terminal truncated beta amyloids by NMR. ACS Chem Neurosci 8(4):759–765. https://doi.org/10.1021/acschemneuro.6b00456
8. Harigaya Y, Saido TC, Eckman CB, Prada CM, Shoji M, Younkin SG (2000) Amyloid beta protein starting pyroglutamate at position 3 is a major component of the amyloid deposits in the Alzheimer's disease brain. Biochem Biophys Res Commun 276(2):422–427. https://doi.org/10.1006/bbrc.2000.3490
9. Piechotta A, Parthier C, Kleinschmidt M, Gnoth K, Pillot T, Lues I, Demuth HU, Schilling S et al (2017) Structural and functional analyses of pyroglutamate-amyloid-beta-specific antibodies as a basis for Alzheimer immunotherapy. J Biol Chem 292(30):12713–12724. https://doi.org/10.1074/jbc.M117.777839
10. Dammers C, Schwarten M, Buell AK, Willbold D (2017) Pyroglutamate-modified Aβ(3-42) affects aggregation kinetics of Aβ(1-42) by accelerating primary and secondary pathways. Chem Sci 8:8–5004. https://doi.org/10.1039/c6sc04797a
11. Smith LM, Strittmatter SM (2017) Binding sites for amyloid-beta oligomers and synaptic toxicity. Cold Spring Harb Perspect Med 7(5). https://doi.org/10.1101/cshperspect.a024075
12. Stahl N, Borchelt DR, Hsiao K, Prusiner SB (1987) Scrapie prion protein contains a phosphatidylinositol glycolipid. Cell 51(2):229–240
13. Balducci C, Beeg M, Stravalaci M, Bastone A, Sclip A, Biasini E, Tapella L, Colombo L et al (2010) Synthetic amyloid-beta oligomers impair long-term memory independently of cellular prion protein. Proc Natl Acad Sci U S A 107(5):2295–2300. https://doi.org/10.1073/pnas.0911829107
14. Larson M, Sherman MA, Amar F, Nuvolone M, Schneider JA, Bennett DA, Aguzzi A, Lesne SE (2012) The complex PrP(c)-Fyn couples human oligomeric Abeta with pathological tau changes in Alzheimer's disease. J Neurosci 32(47):16857–16871a. https://doi.org/10.1523/JNEUROSCI.1858-12.2012
15. Salazar SV, Strittmatter SM (2017) Cellular prion protein as a receptor for amyloid-beta oligomers in Alzheimer's disease. Biochem Biophys Res Commun 483(4):1143–1147. https://doi.org/10.1016/j.bbrc.2016.09.062
16. Zhou J, Liu B (2013) Alzheimer's disease and prion protein. Intractable Rare Dis Res 2(2):35–44. https://doi.org/10.5582/irdr.2013.v2.2.35
17. Beraldo FH, Ostapchenko VG, Caetano FA, Guimaraes AL, Ferretti GD, Daude N, Bertram L, Nogueira KO et al (2016) Regulation of amyloid beta oligomer binding to neurons and neurotoxicity by the prion protein-mGluR5 complex. J Biol Chem 291(42):21945–21955. https://doi.org/10.1074/jbc.M116.738286
18. Linden R (2017) The biological function of the prion protein: a cell surface scaffold of signaling modules. Front Mol Neurosci 10:77. https://doi.org/10.3389/fnmol.2017.00077
19. Lauren J, Gimbel DA, Nygaard HB, Gilbert JW, Strittmatter SM (2009) Cellular prion protein mediates impairment of synaptic plasticity by amyloid-beta oligomers. Nature 457(7233):1128–1132. https://doi.org/10.1038/nature07761
20. Nieznanski K, Choi JK, Chen S, Surewicz K, Surewicz WK (2012) Soluble prion protein inhibits amyloid-beta (Abeta) fibrillization and toxicity. J Biol Chem 287(40):33104–33108. https://doi.org/10.1074/jbc.C112.400614
21. Scott-McKean JJ, Surewicz K, Choi JK, Ruffin VA, Salameh AI, Nieznanski K, Costa AC, Surewicz WK (2016) Soluble prion protein and its N-terminal fragment prevent impairment of synaptic plasticity by Abeta oligomers: implications for novel therapeutic strategy in Alzheimer's disease. Neurobiol Dis 91:124–131. https://doi.org/10.1016/j.nbd.2016.03.001
22. Cohen ML, Kim C, Haldiman T, ElHag M, Mehndiratta P, Pichet T, Lissemore F, Shea M et al (2015) Rapidly progressive Alzheimer's disease features distinct structures of amyloid-beta. Brain 138(Pt 4):1009–1022. https://doi.org/10.1093/brain/awv006
23. Xue C, Lin TY, Chang D, Guo Z (2017) Thioflavin T as an amyloid dye: fibril quantification, optimal concentration and effect on aggregation. R Soc Open Sci 4(1):160696. https://doi.org/10.1098/rsos.160696
24. Liu G, Gaines JC, Robbins KJ, Lazo ND (2012) Kinetic profile of amyloid formation in the presence of an aromatic inhibitor by nuclear magnetic resonance. ACS Med Chem Lett 3(10):856–859. https://doi.org/10.1021/ml300147m
25. Galante D, Corsaro A, Florio T, Vella S, Pagano A, Sbrana F, Vassalli M, Perico A et al (2012) Differential toxicity, conformation and morphology of typical initial aggregation states of Abeta1-42 and Abetapy3-42 beta-amyloids. Int J Biochem Cell Biol 44(11):2085–2093. https://doi.org/10.1016/j.biocel.2012.08.010
26. Hung LW, Ciccotosto GD, Giannakis E, Tew DJ, Perez K, Masters CL, Cappai R, Wade JD et al (2008) Amyloid-beta peptide (Abeta) neurotoxicity is modulated by the rate of peptide aggregation: Abeta dimers and trimers correlate with neurotoxicity. J Neurosci 28(46):11950–11958. https://doi.org/10.1523/JNEUROSCI.3916-08.2008
27. Nielsen L, Khurana R, Coats A, Frokjaer S, Brange J, Vyas S, Uversky VN, Fink AL (2001) Effect of environmental factors on the kinetics of insulin fibril formation: elucidation of the molecular mechanism. Biochemistry 40(20):6036–6046
28. Broersen K, Jonckheere W, Rozenski J, Vandersteen A, Pauwels K, Pastore A, Rousseau F, Schymkowitz J (2011) A standardized and biocompatible preparation of aggregate-free amyloid beta peptide for biophysical and biological studies of Alzheimer's disease. Protein Eng Des Sel 24(9):743–750. https://doi.org/10.1093/protein/gzr020
29. Pauwels K, Williams TL, Morris KL, Jonckheere W, Vandersteen A, Kelly G, Schymkowitz J, Rousseau F et al (2012) Structural basis for increased toxicity of pathological abeta42: abeta40 ratios in Alzheimer disease. J Biol Chem 287(8):5650–5660. https://doi.org/10.1074/jbc.M111.264473
30. Sklenar V, Piotto M, Leppik R, Saudek V (1993) Gradient-tailored water suppression for H-1-N-15 Hsqc experiments optimized to retain full sensitivity. J Magn Reson Ser A 102(2):241–245. https://doi.org/10.1006/jmra.1993.1098
31. Mori S, Abeygunawardana C, Johnson MO, Vanzijl PCM (1995) Improved sensitivity of HSQC spectra of exchanging protons at short interscan delays using a new fast HSQC (FHSQC) detection scheme that avoids water saturation. J Magn Reson Ser B 108(1):94–98. https://doi.org/10.1006/jmrb.1995.1109
32. Ikura M, Bax A (1992) Isotope-filtered 2d NMR of a protein peptide complex: study of a skeletal-muscle myosin light chain kinase fragment bound to calmodulin. J Am Chem Soc 114(7):2433–2440. https://doi.org/10.1021/ja00033a019
33. Delaglio F, Grzesiek S, Vuister GW, Zhu G, Pfeifer J, Bax A (1995) NMRPipe: a multidimensional spectral processing system based on UNIX pipes. J Biomol NMR 6(3):277–293
34. Johnson BA (2004) Using NMRView to visualize and analyze the NMR spectra of macromolecules. Methods Mol Biol 278:313–352. https://doi.org/10.1385/1-59259-809-9:313
35. Gentile MT, Nawa Y, Lunardi G, Florio T, Matsui H, Colucci-D'Amato L (2012) Tryptophan hydroxylase 2 (TPH2) in a neuronal cell line: modulation by cell differentiation and NRSF/rest activity. J Neurochem 123(6):963–970. https://doi.org/10.1111/jnc.12004
36. Corsaro A, Bajetto A, Thellung S, Begani G, Villa V, Nizzari M, Pattarozzi A, Solari A et al (2016) Cellular prion protein controls

stem cell-like properties of human glioblastoma tumor-initiating cells. Oncotarget 7(25):38638–38657. https://doi.org/10.18632/oncotarget.9575

37. Villa V, Thellung S, Bajetto A, Gatta E, Robello M, Novelli F, Tasso B, Tonelli M et al (2016) Novel celecoxib analogues inhibit glial production of prostaglandin E2, nitric oxide, and oxygen radicals reverting the neuroinflammatory responses induced by misfolded prion protein fragment 90-231 or lipopolysaccharide. Pharmacol Res 113(Pt A):500–514. https://doi.org/10.1016/j.phrs.2016.09.010
38. Thellung S, Gatta E, Pellistri F, Villa V, Corsaro A, Nizzari M, Robello M, Florio T (2017) Different molecular mechanisms mediate direct or glia-dependent prion protein fragment 90-231 neurotoxic effects in cerebellar granule neurons. Neurotox Res 32:381–397. https://doi.org/10.1007/s12640-017-9749-2
39. Villa V, Thellung S, Corsaro A, Novelli F, Tasso B, Colucci-D'Amato L, Gatta E, Tonelli M et al (2016) Celecoxib inhibits prion protein 90-231-mediated pro-inflammatory responses in microglial cells. Mol Neurobiol 53(1):57–72. https://doi.org/10.1007/s12035-014-8982-4
40. Lauren J (2014) Cellular prion protein as a therapeutic target in Alzheimer's disease. J Alzheimers Dis 38(2):227–244. https://doi.org/10.3233/JAD-130950
41. Corsaro A, Thellung S, Villa V, Nizzari M, Florio T (2012) Role of prion protein aggregation in neurotoxicity. Int J Mol Sci 13(7):8648–8669. https://doi.org/10.3390/ijms13078648
42. Zou WQ, Capellari S, Parchi P, Sy MS, Gambetti P, Chen SG (2003) Identification of novel proteinase K-resistant C-terminal fragments of PrP in Creutzfeldt-Jakob disease. J Biol Chem 278(42):40429–40436. https://doi.org/10.1074/jbc.M308550200
43. Dammers C, Gremer L, Neudecker P, Demuth HU, Schwarten M, Willbold D (2015) Purification and characterization of recombinant N-terminally pyroglutamate-modified amyloid-beta variants and structural analysis by solution NMR spectroscopy. PLoS One 10(10):e0139710. https://doi.org/10.1371/journal.pone.0139710
44. Wulff M, Baumann M, Thummler A, Yadav JK, Heinrich L, Knupfer U, Schlenzig D, Schierhorn A et al (2016) Enhanced fibril fragmentation of N-terminally truncated and pyroglutamyl-modified Abeta peptides. Angew Chem Int Ed Engl 55(16):5081–5084. https://doi.org/10.1002/anie.201511099
45. Scheidt HA, Adler J, Krueger M, Huster D (2016) Fibrils of truncated pyroglutamyl-modified Abeta peptide exhibit a similar structure as wildtype mature Abeta fibrils. Sci Rep 6:33531. https://doi.org/10.1038/srep33531
46. Schilling S, Lauber T, Schaupp M, Manhart S, Scheel E, Bohm G, Demuth HU (2006) On the seeding and oligomerization of pGlu-amyloid peptides (in vitro). Biochemistry 45(41):12393–12399. https://doi.org/10.1021/bi0612667
47. Younan ND, Sarell CJ, Davies P, Brown DR, Viles JH (2013) The cellular prion protein traps Alzheimer's Abeta in an oligomeric form and disassembles amyloid fibers. FASEB J 27(5):1847–1858. https://doi.org/10.1096/fj.12-222588
48. Bove-Fenderson E, Urano R, Straub JE, Harris DA (2017) Cellular prion protein targets amyloid-beta fibril ends via its C-terminal domain to prevent elongation. J Biol Chem 292:16858–16871. https://doi.org/10.1074/jbc.M117.789990
49. Suvorina MY, Selivanova OM, Grigorashvili EI, Nikulin AD, Marchenkov VV, Surin AK, Galzitskaya OV (2015) Studies of polymorphism of amyloid-beta42 peptide from different suppliers. J Alzheimers Dis 47(3):583–593. https://doi.org/10.3233/JAD-150147
50. Editorial NN (2011) State of aggregation. Nat Neurosci 14(4):399. https://doi.org/10.1038/nn0411-399
51. Fawzi NL, Ying J, Ghirlando R, Torchia DA, Clore GM (2011) Atomic-resolution dynamics on the surface of amyloid-beta protofibrils probed by solution NMR. Nature 480(7376):268–272. https://doi.org/10.1038/nature10577
52. Algamal M, Ahmed R, Jafari N, Ahsan B, Ortega J, Melacini G (2017) Atomic-resolution map of the interactions between an amyloid inhibitor protein and amyloid beta (Abeta) peptides in the monomer and protofibril states. J Biol Chem 292(42):17158–17168. https://doi.org/10.1074/jbc.M117.792853
53. Cremades N, Dobson CM (2018) The contribution of biophysical and structural studies of protein self-assembly to the design of therapeutic strategies for amyloid diseases. Neurobiol Dis 109(Pt B):178–190. https://doi.org/10.1016/j.nbd.2017.07.009
54. Cohen SI, Linse S, Luheshi LM, Hellstrand E, White DA, Rajah L, Otzen DE, Vendruscolo M et al (2013) Proliferation of amyloid-beta42 aggregates occurs through a secondary nucleation mechanism. Proc Natl Acad Sci U S A 110(24):9758–9763. https://doi.org/10.1073/pnas.1218402110
55. Ganzinger KA, Narayan P, Qamar SS, Weimann L, Ranasinghe RT, Aguzzi A, Dobson CM, McColl J et al (2014) Single-molecule imaging reveals that small amyloid-beta1-42 oligomers interact with the cellular prion protein (PrP(C)). Chembiochem 15(17):2515–2521. https://doi.org/10.1002/cbic.201402377
56. Tomaselli S, Esposito V, Vangone P, van Nuland NA, Bonvin AM, Guerrini R, Tancredi T, Temussi PA et al (2006) The alpha-to-beta conformational transition of Alzheimer's Abeta-(1-42) peptide in aqueous media is reversible: a step by step conformational analysis suggests the location of beta conformation seeding. Chembiochem 7(2):257–267. https://doi.org/10.1002/cbic.200500223
57. Schmidt M, Rohou A, Lasker K, Yadav JK, Schiene-Fischer C, Fandrich M, Grigorieff N (2015) Peptide dimer structure in an Abeta (1-42) fibril visualized with cryo-EM. Proc Natl Acad Sci U S A 112(38):11858–11863. https://doi.org/10.1073/pnas.1503455112
58. Colvin MT, Silvers R, Ni QZ, Can TV, Sergeyev I, Rosay M, Donovan KJ, Michael B et al (2016) Atomic resolution structure of monomorphic Abeta42 amyloid fibrils. J Am Chem Soc 138(30):9663–9674. https://doi.org/10.1021/jacs.6b05129
59. Galante D, Ruggeri FS, Dietler G, Pellistri F, Gatta E, Corsaro A, Florio T, Perico A et al (2016) A critical concentration of N-terminal pyroglutamylated amyloid beta drives the misfolding of Ab1-42 into more toxic aggregates. Int J Biochem Cell Biol 79:261–270. https://doi.org/10.1016/j.biocel.2016.08.037
60. Corsaro A, Paludi D, Villa V, D'Arrigo C, Chiovitti K, Thellung S, Russo C, Di Cola D et al (2006) Conformation dependent pro-apoptotic activity of the recombinant human prion protein fragment 90-231. Int J Immunopathol Pharmacol 19(2):339–356. https://doi.org/10.1177/039463200601900211
61. Chiovitti K, Corsaro A, Thellung S, Villa V, Paludi D, D'Arrigo C, Russo C, Perico A et al (2007) Intracellular accumulation of a mild-denatured monomer of the human PrP fragment 90-231, as possible mechanism of its neurotoxic effects. J Neurochem 103(6):2597–2609. https://doi.org/10.1111/j.1471-4159.2007.04965.x
62. Fluharty BR, Biasini E, Stravalaci M, Sclip A, Diomede L, Balducci C, La Vitola P, Messa M et al (2013) An N-terminal fragment of the prion protein binds to amyloid-beta oligomers and inhibits their neurotoxicity in vivo. J Biol Chem 288(11):7857–7866. https://doi.org/10.1074/jbc.M112.423954
63. Goldblatt G, Cilenti L, Matos JO, Lee B, Ciaffone N, Wang QX, Tetard L, Teter K et al (2017) Unmodified and pyroglutamylated amyloid beta peptides form hypertoxic hetero-oligomers of unique secondary structure. FEBS J 284(9):1355–1369. https://doi.org/10.1111/febs.14058
64. Audano M, Schneider A, Mitro N (2018) Mitochondria, lysosomes and dysfunction: their meaning in neurodegeneration. J Neurochem. https://doi.org/10.1111/jnc.14471
65. Thellung S, Corsaro A, Villa V, Simi A, Vella S, Pagano A, Florio T (2011) Human PrP90-231-induced cell death is associated with

intracellular accumulation of insoluble and protease-resistant macroaggregates and lysosomal dysfunction. Cell Death Dis 2:e138. https://doi.org/10.1038/cddis.2011.21

66. Thellung S, Scoti B, Corsaro A, Villa V, Nizzari M, Gagliani MC, Porcile C, Russo C et al (2018) Pharmacological activation of autophagy favors the clearing of intracellular aggregates of misfolded prion protein peptide to prevent neuronal death. Cell Death Dis 9(2):166. https://doi.org/10.1038/s41419-017-0252-8
67. Um JW, Nygaard HB, Heiss JK, Kostylev MA, Stagi M, Vortmeyer A, Wisniewski T, Gunther EC et al (2012) Alzheimer amyloid-beta oligomer bound to postsynaptic prion protein activates Fyn to impair neurons. Nat Neurosci 15(9):1227–1235. https://doi.org/10.1038/nn.3178
68. Um JW, Kaufman AC, Kostylev M, Heiss JK, Stagi M, Takahashi H, Kerrisk ME, Vortmeyer A et al (2013) Metabotropic glutamate receptor 5 is a coreceptor for Alzheimer abeta oligomer bound to cellular prion protein. Neuron 79(5):887–902. https://doi.org/10.1016/j.neuron.2013.06.036
69. Ahmed R, Melacini G (2018) A solution NMR toolset to probe the molecular mechanisms of amyloid inhibitors. Chem Commun (Camb) 54(37):4644–4652. https://doi.org/10.1039/c8cc01380b
70. Ahmed M, Davis J, Aucoin D, Sato T, Ahuja S, Aimoto S, Elliott JI, Van Nostrand WE et al (2010) Structural conversion of neurotoxic amyloid-beta(1-42) oligomers to fibrils. Nat Struct Mol Biol 17(5):561–567. https://doi.org/10.1038/nsmb.1799
71. Milojevic J, Esposito V, Das R, Melacini G (2007) Understanding the molecular basis for the inhibition of the Alzheimer's Abeta-peptide oligomerization by human serum albumin using saturation transfer difference and off-resonance relaxation NMR spectroscopy. J Am Chem Soc 129(14):4282–4290. https://doi.org/10.1021/ja067367+
72. Garai K, Frieden C (2013) Quantitative analysis of the time course of Abeta oligomerization and subsequent growth steps using tetramethylrhodamine-labeled Abeta. Proc Natl Acad Sci U S A 110(9):3321–3326. https://doi.org/10.1073/pnas.1222478110